

Geometrical Analysis of Parabolic Trough Solar Collector

Mohamed Salim Djenane, Seddik Hadji, and Omar Touhami

Abstract—The geometric of the parabolic trough collector (PTC) is a field that should be paid special attention, knowing that a better geometry induces a better efficiency and lower costs. Nowadays, many types of geometry exist, such as LS-2, LS-3, Euro trough, ENEA, SGX-2, Sener trough, Helio trough, Sky trough, Ultimate trough. This paper deals with a geometrical analysis of PTC. The analysis is based on the coefficient of deviation angle to highlight the effect of PTC (LS-2) parameters on the optical efficiency. The effects of focal length, tube diameter, and collector width on the coefficient of deviation angle have been considered using a two-dimensional problem, and the simulation has been done employing MATLAB software. The derived results confirm that the tube diameter is the parameter most influencing compared to the other parameters. In addition, the width and length of the Euro trough, Helio trough, and Ultimate trough were considered to simulate thermal efficiency. The best observed performance is that of the Ultimate trough, which presents a 2% higher difference in efficiency and also represents a better size, which allows reducing the number of units to be assembled in the solar field. That leads to reducing the count of motors, sensors, connection joints, foundations, controllers, pylons.

Keywords—Parabolic trough, Geometric, Coefficient of deviation angle, Efficiency.

NOMENCLATURE

β : Deviation angle (*degree*).
 d : Tube diameter (*m*).
 f : Focal length (*m*).
 B : Collector's width (*m*).
 A_a : Aperture Area of the mirror (*m*²).
 A_{ro} : Receiver outer area (*m*²).
 A_{ri} : Receiver inner area (*m*²).
 L : Collector length (*m*).
 D_{ri} : Receiver inner diameter (*m*).
 D_{ro} : Receiver outer diameter (*m*).
 D_{ci} : Cover inner diameter (*m*).
 D_{co} : Cover outer diameter (*m*).
 T : Temperature (*K*).
 C_p : Specific heat capacity (*Jkg*⁻¹*K*⁻¹).
 T_{am} : Ambient temperature (*K*).
 μ : Dynamic viscosity.
 k : Thermal conductivity (*Wm*⁻¹*K*⁻¹).
 ρ : Density (*kg/m*³).
 m : Mass flow rate (*kg/s*).
 Re : Reynolds number.
 Pr : Prandtl number.
 Nu : Nusselt number.
 h : Heat transfer coefficient fluid/absorber (*w/m*²*K*).
 h_{out} : Heat transfer coefficient cover/environment (*w/m*²*K*).
 σ : Stefan Boltzmann constant.

Manuscript received February 7, 2024; revised July 12, 2024.

M.S. Djenane and O. Touhami is with the Electrical Engineering Department, Ecole Nationale Polytechnique, Algiers, ALGERIA (e-mail: mohamed_salim.djenane@g.enp.edu.dz, omar.touhami@g.enp.edu.dz).

S. Hadji is with the Electrical Engineering Department, Ecole Nationale Polytechnique, and Ecole Supérieure des Sciences Appliquées, Algiers, ALGERIA (e-mail: seddik.hadji@g.essaa.edu.dz).

Digital Object Identifier (DOI): 10.53907/enpesj.v4i2.258

I. INTRODUCTION

Nowadays, the main primary sources used in power plants are fossil fuels. Unfortunately, these raise major ecological concerns. They represent exhaustible sources of energy and constitute reservoirs of toxic wastes. There is also the risk linked to radioactivity in nuclear power plants. The world is then moving towards the solution of exploiting renewables energies to remedy these problems [1]. Among renewable energies, solar energy is the most used source for producing electricity, especially through CSP (Concentrated Solar Power) systems. Among CSP systems is found the parabolic trough system, which is the most successful worldwide [2], as many parabolic trough solar power plants are built in many countries such as the USA, Spain, Morocco, Algeria.

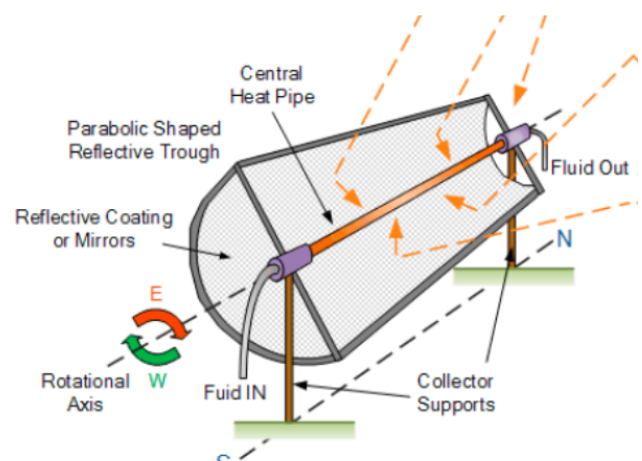


Fig. 1: Parabolic Trough Collector basic elements [15]

Many works have been carried out focusing on the geometrical shape of parabolic trough solar collector [3-5]. The geometrical modifications are done on absorber tubes to improve the PTC's

performance such as the circular-trapezoidal absorber tube [6], sinusoidal absorber tube [7], and helicoidal absorber tube [8]. Also, a modification is introduced inside the absorber tube, as seen in Single-sided spiral ribbed absorber tube [9], and in absorber tube with pin fin array insertion [10]. In addition, geometrical analyses have been done on PTC, among which the geometric optimization based on the local concentration ratio using the Monte Carlo method [11], and also on the optical performance employing particle swarm optimization algorithm [12]. An optics and thermodynamics analysis have been carried out on several configurations, considering the concentrating ratio and cost factor [13]. However, changes are simultaneously made in the internal and external geometry of the receiving tube in [14].

In this paper, the variation of the coefficient of deviation angle is considered in view of simulating the effect of focal length, tube diameter and collector's width on the optical efficiency of PTC (LS-2). These effects are determined as a function of deviation angle. Then an interpretation is performed showing that the tube diameter influences the optical efficiency more than the focal length and collector's width. Moreover, Euro trough, Helio trough, Ultimate trough are examined to highlight the effects of aperture area and tube diameter length. The Ultimate Trough is the most efficient type regarding the thermal efficiency.

This paper is organized in six sections: The parabolic trough collector is presented in section II. Then the coefficient of deviation angle is studied in section III, showing the effects of focal length, tube diameter, and collector's width (Section IV). Section V is devoted to thermal efficiency considering Euro trough, Helio trough, and Ultimate trough types. Finally, the conclusions of this work are presented in section VI.

II. PARABOLIC TROUGH COLLECTOR

Parabolic trough collector is conceived by a long mirror in parabolic shape, an absorber tube placed at the focal line of the collector, in which a heat transfer fluid flows (Fig. 1). Glasses to reduce heat losses by convection cover the absorber tube. The PTC is attached to a support and a system assuring the tracking of the sun.

The parabolic trough types considered in this study are: LS-2, Euro trough, Helio trough and Ultimate trough, focusing on the geometrical analysis.

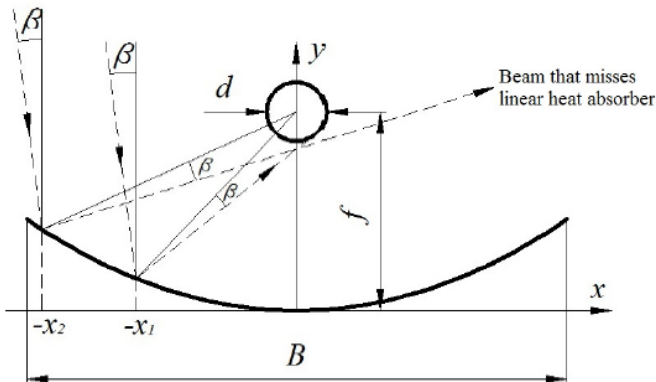


Fig. 2: Small deviation of incidence angle of sun beam at parabolic trough collector [16]

III. COEFFICIENT OF DEVIATION ANGLE

The coefficient of deviation angle depends on the deviation angle (η_β), it takes into account the decrease in thermal performance due to small deviation angle between the solar beam and focal plane. The small deviation of incidence angle of sun beam at parabolic trough collector is shown in Fig. 2.

Figure 2 shows a cross section of parabolic trough collector on which can be seen the effect of small deviation angle, the rays coming onto the collector at the point with the coordinate $-x_2$ can not reach the absorber tube and is lost. Also the rays with coordinates $(-x_i; i > 2)$ can not reach the absorber tube neither. It can be observed that at each point of collector there is a defined interval of the deviation angle $[\beta_{min}; \beta_{max}]$ where the rays reach the absorber tube. After analyzing this two dimensional problem, the coefficient of deviation angle η_β can be defined as, [16, 17]:

$$\eta_\beta = \begin{cases} 1, & \beta \leq \beta_{min} \\ \frac{4f}{B} \sqrt{\frac{d}{2f \sin(\beta)} - 1}, & \beta_{min} \leq \beta \leq \beta_{max} \\ 0, & \beta \leq \beta_{max} \end{cases} \quad (1)$$

with β_{min} and β_{max} being determined as, [5]:

$$\beta_{min} = \arcsin\left(\frac{8fd}{16f^2 + B^2}\right) \quad (2)$$

$$\beta_{max} = \arcsin\left(\frac{d}{f}\right) \quad (3)$$

Figure 3 shows the variation of the coefficient of deviation angle versus deviation angle (β , radians), obtained for $B = 2.75m$; $f = 0.81m$ and $d = 0.04m$.

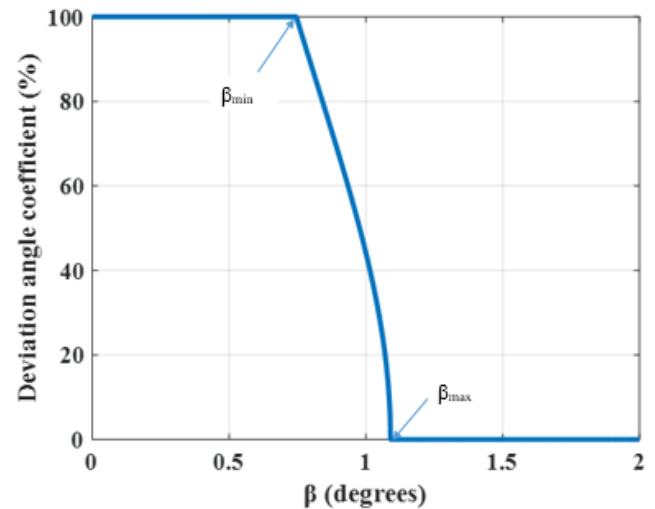


Fig. 3: variation of the coefficient of deviation angle versus the deviation angle

It is to be noted that, actually, the interval of deviation angle (β) referred to above represents the concentrator's operating margin, i.e. it exhibits a significant efficiency within this margin, particularly when approaching β_{min} . So, the concentrator should be better operated from 0 to β_{max} .

IV. EFFECT OF PARABOLIC TROUGH PARAMETERS ON THE COEFFICIENT OF DEVIATION ANGLE

A. Effect of focal length

To evaluate the influence of the focal length on the coefficient of deviation angle, the collector’s width and tube diameter are fixed and the focal length is varied. The shape of the collector evolves as shows Fig. 3, and the variation of the coefficient of deviation angle is shown in Fig. 4. The equation of the parabola is given by Eq. (4).

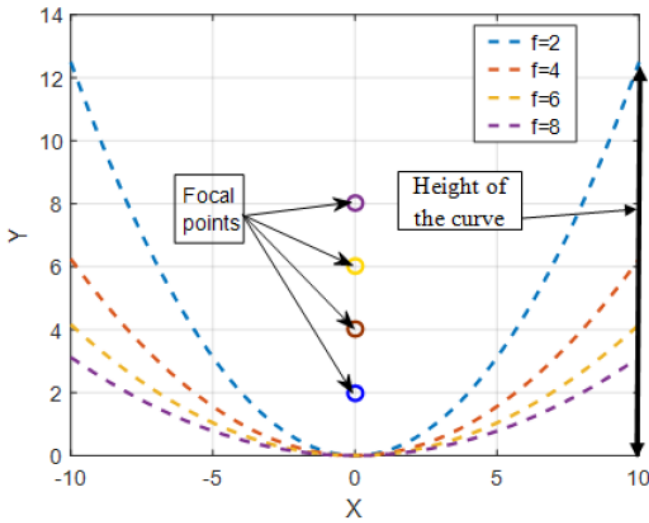


Fig. 4: variation of the collector shape versus coordinate x with the focal length as a parameter.

$$Y(x) = \frac{x^2}{4f} \tag{4}$$

Figure 4 is obtained by varying the focal length for the following values: 2m, 4m, 6m and 8m. It can be observed that the more the focal length is increased the more the width decreases and consequently the collector’s area decreases and the costs decrease as well.

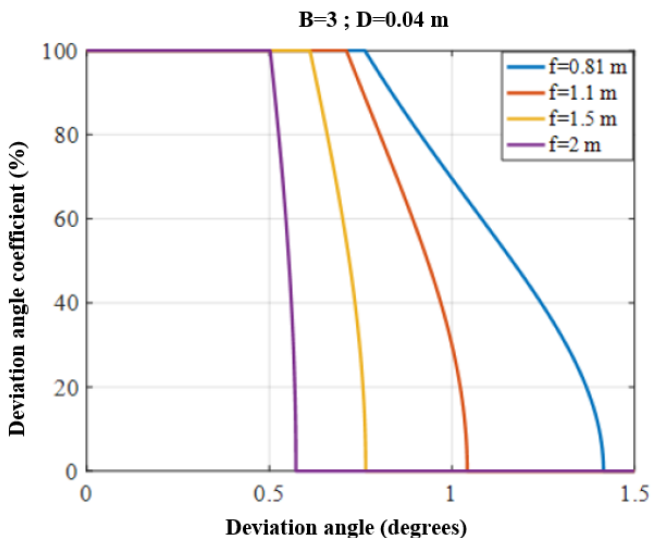


Fig. 5: Variation of the coefficient of deviation versus deviation angle with the focal length as a parameter.

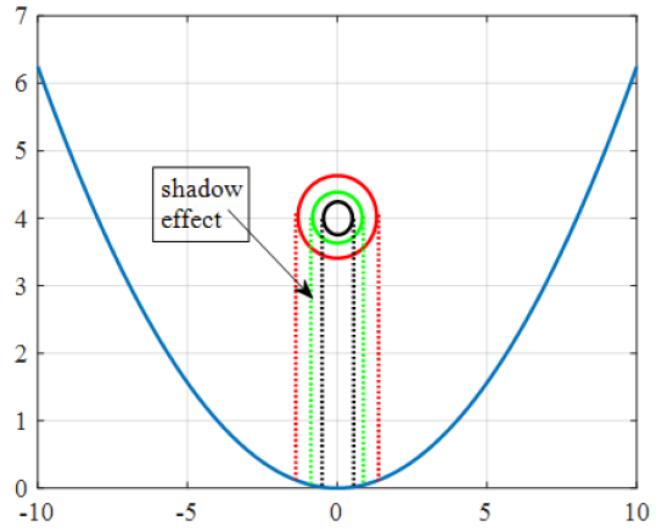


Fig. 6: Shadow effect with variation of tube diameter

The plot relative to the evolution of the coefficient of deviation angle versus the deviation angle with the focal length as a parameter is shown in Fig. 5. From this latter, it can be seen that the operating margin of the concentrator (within which the solar rays reach the absorber tube) goes larger as the focal length becomes smaller. And when the margin is large it means that the angle of incidence has a large margin of variation, For example, comparing for $f_1 = 0.81m$ and $f_2 = 1.1m$, gives for: $f_2 = 1.1m$, $\beta = 1$ degree, and $\eta_\beta = 29.95\%$, and for $f_1 = 0.81m$, $\beta = 1.314$, and $\eta_\beta = 29.95\%$, i.e. the same value of the coefficient of deviation angle η_β for both the focal length values. Note that the margin $[1.314; \beta_{max-f_1}]$ is higher compared to $[1; \beta_{max} - f_2]$. In other words, $0.101degrees > 0.042degrees$.

Now assume the effect of wind or an inaccuracy in the tracking system exists. Then at a given moment the concentrator changes its position which causes a change in the angle of incidence of 0.042 degrees implying that $\eta_{\beta-f_2} = 0\%$ against $\eta_{\beta-f_1} = 22.58\%$. So, it is beneficial to work adopting a large margin. However, lowering the focal point involves increasing the aperture area and, subsequently, increasing the costs.

B. Effect of tube diameter

To see the influence of the tube diameter on the coefficient of deviation angle, the collector’s width and focal length are fixed and the tube diameter is varied.

Figure 6 shows the shadow effect due to the increase of the tube diameter.

It can be seen that if the diameter of the absorber tube is increased, the shadow area at the surface of the collector increases and then the corresponding materials do not contribute to the reflection process thus causing an increase in the costs. On the other hand, it is advantageous to increase the tube diameter, as shown in Fig. 7. This latter shows the variations of the coefficient of deviation angle with the tube diameter (d) as a parameter for the following values of ($d = 0.04m; d = 0.06m; d = 0.08m$ and $d = 0.1m$).

It can be seen that the increase in diameter of the receiver (d) increases the margin within which the rays reach the absorber

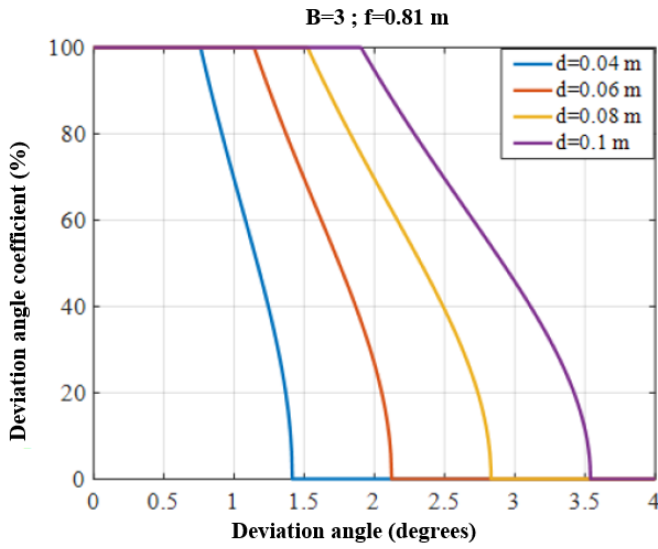


Fig. 7: Variation of the coefficient of deviation angle versus deviation angle with the tube diameter as a parameter.

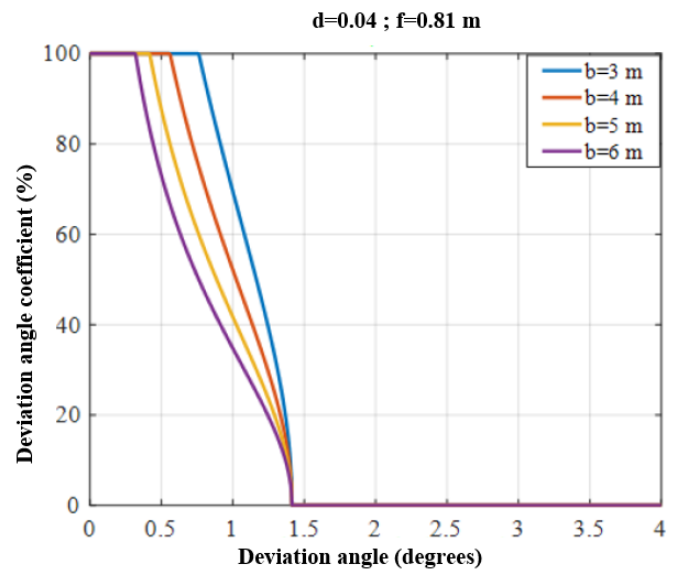


Fig. 9: Variation of the coefficient of deviation angle versus deviation angle with the collector's width as a parameter.

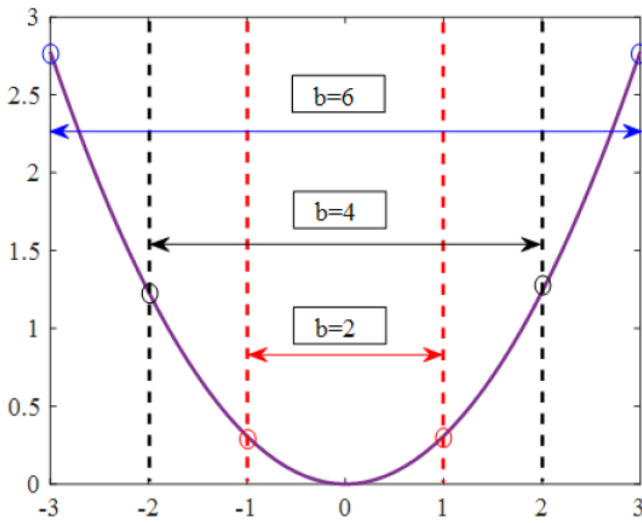


Fig. 8: Variation of collector's width

tube.

C. Effect of collector's width

Proceeding the same way, to see the influence of the collector's width on the coefficient of deviation angle, the tube diameter and focal length are fixed and the collector's width is varied. Figure 8 is obtained for the following values of the collector's width: 2m, 4m and 6m.

It can be seen from Fig. 8 that if the collector's width is increased, a larger sensing section is obtained, but still remains the disadvantage related to the costs. The variations of the coefficient of deviation angle against the collector's width are shown in Fig. 9. From this latter, it appears that the collector's width does not affect β_{max} but influences β_{min} . The variation of the coefficient of deviation angle according collector's width is given by Fig. 9. So, the increase of (B) decreases β_{min} , which increases the margin of variation of β , and that because of the increase in the collector's area.

V. THERMAL ANALYSIS

In this section, three types of parabolic trough collector are examined, the Euro trough, Helio trough, and Ultimate trough, to highlight the effect of the geometry of the collector on the thermal efficiency.

The three types are considered here as conceived with the same materials, the only one difference being in the collector's area.

The energy balanced model is used to simulate the thermal efficiency. The different heat modes are represented in Fig.10 while the Euro trough, Helio trough and Ultimate trough are represented in Fig. 11.

The solar energy comes onto the collector, then will be reflected towards the absorber tube, and the heat will be transferred to the heat transfer fluid with some losses that should be considered.

The heat coming onto the collector can be expressed as, Eq. (5).

$$Q_s = A_a * G_b \quad (5)$$

The useful heat absorbed by the heat transfer fluid is determined by Eq. (6).

$$Q_u = mC_p(T_{out} - T_{in}) \quad (6)$$

And the heat losses are determined by Eq. (7).

$$Q_{loss} = h_{out}A_{co}(T_c - T_{am}) + A_{co}\sigma\epsilon_c(T_c^4 - T_{am}^4) \quad (7)$$

The useful heat can then be written as follows :

$$Q_u = Q_s\eta_{op} - Q_{loss} \quad (8)$$

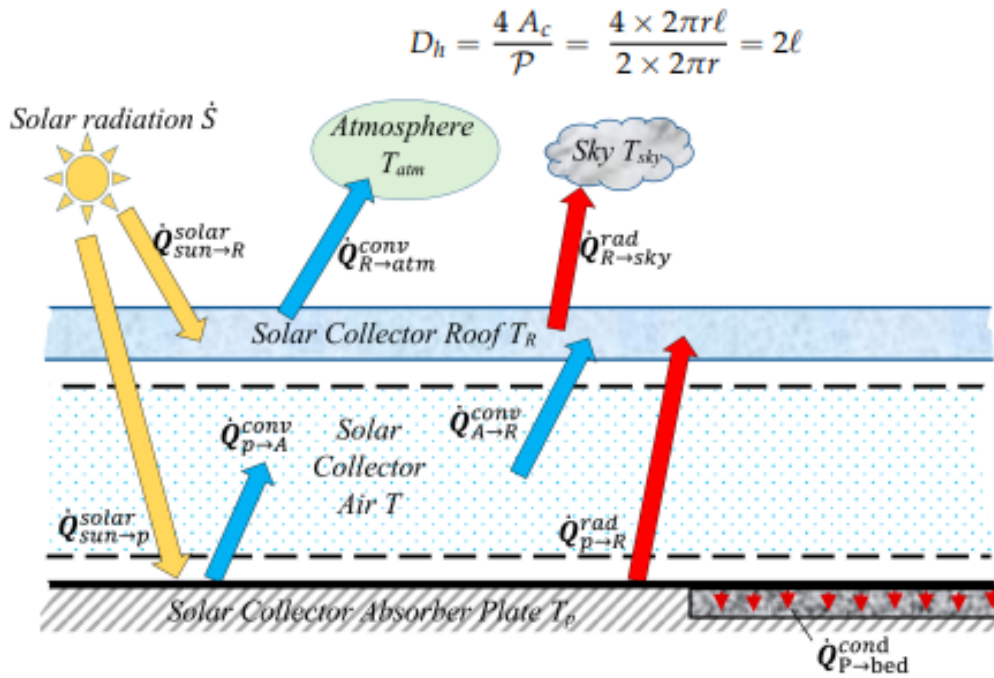


Fig. 10: Heat transfert modes [18]

Which is rewritten as a function of receiver temperature as (Eq. (9)):

$$Q_u = hA_{ri}(T_r - T_{fm}) \quad (9)$$

$$\rho = 1.2691 * 103 - 1.52115 * T_{am} + (1.79133 * 10^{-3}) * (T_{am}^2) - (1.67145 * 10^{-6}) * (T_{am}^3) \quad (13)$$

Finally, the thermal efficiency is evaluated by Eq. (10).

$$\eta_{th} = \frac{Q_u}{Q_s} \quad (10)$$

And the specific heat capacity is expressed by the following equation :

$$C_p = (1.10787 + (1.70736 * 10^{-3}) * T_{am}) * 1000 \quad (14)$$

The fluid used in this study is the Syltherm 800, its parameters are as defined below :

Finally, the mass flow is determined by Eq. (15).

The dynamic viscosity is determined as follows:

$$m = \rho * V \quad (15)$$

$$\mu = (5.14887 * 10^4 - (9.61656 * 10^2) * T_{am} + 7.50207 * (T_{am}^2) - (3.12468 * 10^{-2}) * (T_{am}^3) + (7.32194 * 10^{-5}) * (T_{am}^4) - (9.14636 * 10^{-8}) * (T_{am}^5) + (4.75624 * 10^{-11}) * (T_{am}^6)) * 10^{-3} \quad (11)$$

Reynolds number, Prandtl number, and Nusselt number are defined successively by Eqs. (16-18).

$$Re = 4 * m / (\Pi * D_{ri} * \mu), \quad (16)$$

$$Pr = \mu * C_p / k, \quad (17)$$

and,

While the thermal conductivity is evaluated as follows :

$$Nu = 0.023 * (Re^{0.8}) * (Pr^{0.4}) \quad (18)$$

$$k = 1.90134 * 10^{-1} - (1.88053 * 10^{-4}) * T_{am} \quad (12)$$

The heat transfer coefficient is then determined by Eq. (19).

On the other hand, the density is expressed as follows :

$$h = (k * Nu) / D_{ri} \quad (19)$$

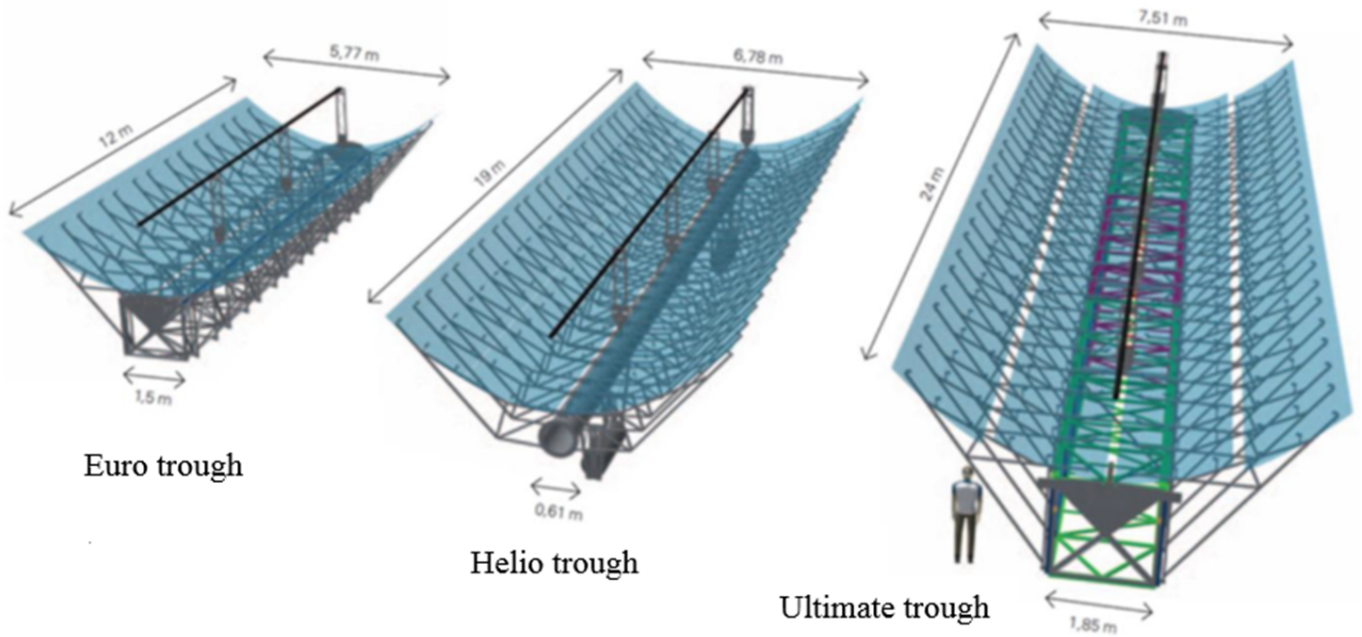


Fig. 11: Euro trough, Helio trough and Ultimate trough collectors [19]

Table. I

EURO TROUGH, HELIO TROUGH, AND ULTIMATE TROUGH PARAMETERS

Parameters	Euro trough	Helio trough	Ultimate trough
A_{am}	69.24 m ²	128.82 m ²	180.24 m ²
A_{ri}	2.487 m ²	3.938 m ²	4.974 m ²
A_{ro}	2.638 m ²	4.1762 m ²	5.257 m ²

And h_{out} is the heat coefficient between the annulus and the ambient, it is defined by Eq. (20).

$$h_{out} = 4 * (V_{wind}^{0.58}) * (D_{co}^{-0.42}) \quad (20)$$

The parameters of simulation that are considered for these types of collector are shown in Table 1.

The results related to the thermal efficiency are shown in Fig. 12 highlighting the difference between the Euro trough, Helio trough and Ultimate trough. The most efficient collector is the Ultimate trough, the less efficient one being the Euro trough, and that depends on the Aperture area, the larger it is the better the efficiency is improved, the difference being more than 2% higher compared to the other ones. The larger aperture area induces the use of more construction materials, but it is to be noted that, on the other hand, the number of assembled collectors is lower. This leads to a reduction in motors, sensors, connection joints, foundations, controllers, pylons, etc. Which in turn reduces the costs of the power plant.

VI. CONCLUSIONS

In this paper, we have highlighted the effects of tube diameter, focal length and collector's width on the coefficient of deviation angle. The variation of tube diameter mainly affects mainly the

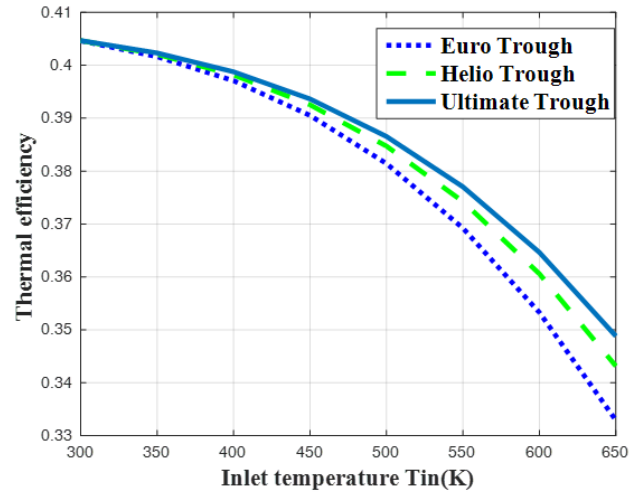


Fig. 12: Thermal efficiencies of Euro trough, Helio trough and Ultimate trough collectors

coefficient of deviation angle. Therefore a compromise must be found between the parabolic trough parameters to reach its right value and thus a high thermal efficiency value and appropriate related economic figures.

The width and the length of Euro trough, Helio trough, and Ultimate trough were examined. The observed best performance was that related to the Ultimate trough, which presents a 2% difference in efficiency, and allows reducing the number of units to be assembled in solar field, i.e. reducing the cost of the power plant.

REFERENCES

- [1] A. Ahmad, O. Prakash, R. Kausher, G. Kumar, S. Pandey, S.M. Hasnain, "Parabolic trough solar collectors: A sustainable and efficient energy source", *Materials Science for Energy Technologies.*, Vol. 7, ISSN 2589-2991, pp. 99–106, 2024. DOI:

- 10.1016/j.mset.2023.08.002.
- [2] E. C. Okonkwo, M. Abid, and T. A.H. Ratlamwala. "Numerical analysis of heat transfer enhancement in a parabolic trough collector based on geometry modifications and working fluid usage." *Journal of Solar Energy Engineering*, Vol. 140, no 5, 051009, 2018.
- [3] L. G.. Fadodun, A. Kaood, M. A. Hassan, "Investigation of the entropy production rate of ferrosioferic oxide/water nanofluid in outward corrugated pipes using a two-phase mixture model", *International Journal of Thermal Sciences*, Vol. 178, 107598, ISSN 1290-0729, 2022 DOI: 10.1016/j.ijthermalsci.2022.107598.
- [4] A. Kaood, G. F. Olatomide, "Numerical investigation of turbulent entropy production rate in conical tubes fitted with a twisted-tape insert", *International Communications in Heat and Mass Transfer*, Vol. 139, 106520, ISSN 0735-1933, 2022 DOI: 10.1016/j.icheatmasstransfer.2022.106520.
- [5] A. Kaood, O. A. Ismail, A.H. Al-Tohamy, "Hydrothermal performance assessment of a parabolic trough with proposed conical solar receiver", *Renewable Energy*, Vol. 222, 119939, ISSN 0960-1481, 2024, DOI: 10.1016/j.renene.2024.119939.
- [6] M. S. Djenane, S. Hadji, O. Touhami, A.H. Zitouni, "A Novel Design of Parabolic Trough Solar Collector's Absorber Tube". *Journal of Solar Energy Engineering*, Vol. 146, no 3, 031001, 2024, DOI: 10.1115/1.4063700.
- [7] Y. Demagh, A. Hachicha, H. Benmoussa, Y. Kabar, "Numerical investigation of a novel sinusoidal tube receiver for parabolic trough technology", *Applied Energy*, Vol. 218, pp.494–510, 2018.
- [8] O. Chakraborty, S. Roy, B. Das, R. Gupta, "Effects of helical absorber tube on the energy and exergy analysis of parabolic solar trough collector—A computational analysis", *Sustainable Energy Technologies and Assessments*, Vol. 44, 101083, 2021.
- [9] B. Zou, Y. Jiang, Y. Yao, H. Yang, "Thermal performance improvement using unilateral spiral ribbed absorber tube for parabolic trough solar collector. *Solar Energy*, Vol. 183, pp.371–38, 2019.
- [10] X. Gong, F. Wang, H. Wang, J. Tan, Q. Lai, H. Han, "Heat transfer enhancement analysis of tube receiver for parabolic trough solar collector with pin fin arrays inserting", *Solar Energy*, Vol.144, pp.185–202, 2017.
- [11] H. Hoseinzadeh, A. Kasaeian, M. Shafii, M. B. "Geometric optimization of parabolic trough solar collector based on the local concentration ratio using the Monte Carlo method", *Energy Conversion and Management*, Vol.175, pp.278–287, 2018.
- [12] Cheng, Z. D., He, Y. L., Du, B. C., Wang, K., Liang, Q. Geometric optimization on optical performance of parabolic trough solar collector systems using particle swarm optimization algorithm. *Applied energy*, 148, 282-293, 2015.
- [13] Behram, Saqib, et al. "Design, fabrication and thermal analysis of parabolic trough collector." *MATEC Web of Conferences, EDP Sciences*, Vol. 398, 2024.
- [14] Peng, Wei, and Omid Karimi Sadaghiani. "Geometrical variation in receiver tube of SEGS LS-2 parabolic trough collector (PTC) based on heat flux distribution to improve the thermal performance." *International Journal of Thermal Sciences* 163, 106858, (2021).
- [15] H. Olia, M. Torabi, M. Bahiraei, M. Ahmadi, M. Goodarzi, M. Safaei, "Application of nanofluids in thermal performance enhancement of parabolic trough solar collector: state-of-the-art", *Applied Sciences*, 9(3), 463, 2019.
- [16] T. Simonović, M. Stamenić, N. Tanasić, M. Trninić, "Effect of small deviation of incident angle on thermal performance of parabolic trough solar collector". In 2016 4th International Symposium on Environmental Friendly Energies and Applications (EFEA) (pp. 1-4). IEEE, 2016.
- [17] M.S. Djenane, S. Hadji, O. Touhami, "Effect of Deviation Angle on the Parabolic Trough Solar Collector Performances," *Proceedings of the 2019 International Conference on Advanced Electrical Engineering (ICAEE)*, Algiers, Algeria, Nov. 19–21, pp. 1–6, 2019.
- [18] H.Z Hassan, "Transient Analysis of a Solar Chimney Power Plant Integrated with a Solid-Sorption Cooling System for Combined Power and Chilled Water Production" *Energies*, 15(18), 6793, 2022.
- [19] C. Caliot, G. Flamant, "Technologie des concentrateurs cylindro-paraboliques", *Laboratoire proceeds, Matériaux et energie solaire, Formation CSP, OUARZAZATE* 25, 27 mai 2016.

Mohamed Salim Djenane is currently Electrical substation engineer at SONELGAZ. He earned his PhD in Electrical Engineering from Ecole Nationale Polytechnique, Algiers in June 2024.

Seddik Hadji is Professor in Electrical Engineering at Ecole Supérieure des Sciences Appliquées, Algiers. His field of expertise is in Power Electronics, Actives Filters and Renewable Energies Solar.

Omar Touhami is a Professor in Electrical Engineering at Ecole Nationale Polytechnique, Algiers. He received the Engineering, M.S., and Ph.D. degrees in electrical engineering from the Ecole Nationale Polytechnique d'Alger, Algiers, Algeria, in 1981, 1986, and 1994, respectively. From 1989 to 1994, he was an Associate Researcher with the Research Center on Automatic of Nancy (CRAN-ENSEM-INPL), where his works on the identification of electric machines were a success in the industries. He has been a Scientific Adviser to the Ministry of Higher Education in Algeria and an Expert Member of the CNEPRU commission since 1997 until 2011. His domains of research are electrical machines, power systems and variable speed drives, and diagnosis of dynamical systems.